forests

MDPI

Article

Allometric Equations for Estimating the Above-Ground Biomass of Five Forest Tree Species in Khangai, Mongolia

Batbaatar Altanzagas [1,2], Yongkai Luo [1], Batbaatar Altansukh [3], Chimidnyam Dorjsuren [3], Jingyun Fang [1,4] and Huifeng Hu [1,*]

1 State Key Laboratory of Vegetation and Environmental Change, Institute of Botany, Chinese Academy of Sciences, Beijing 100093, China
2 International College, University of Chinese Academy of Sciences, Beijing 100049, China
3 Forest Research Laboratory, Institute of General and Experimental Biology, Mongolian Academy of Sciences, Ulaanbaatar 210351, Mongolia
4 College of Urban and Environmental Sciences, and Key Laboratory for Earth Surface Processes of the Ministry of Education, Peking University, No.5 Yiheyuan Rd, Haidian District, Beijing 100871, China
* Correspondence: huifhu@ibcas.ac.cn; Tel.: +86-186-1387-9226

Received: 28 June 2019; Accepted: 5 August 2019; Published: 6 August 2019

Abstract: Understanding the contribution of forest ecosystems to regulating greenhouse gas emissions and maintaining the atmospheric CO_2 balance requires the accurate quantification of above-ground biomass (AGB) at the individual tree species level. The main objective of this study was to develop species-specific allometric equations for the total AGB and various biomass components, including stem, branch, and foliage biomass in Khangai region, northern Mongolia. We destructively sampled a total of 183 trees of five species (22–74 trees per species), including Siberian stone pine (*Pinus sibirica* Du Tour.), Asian white birch (*Betula platyphylla* Sukacz.), Mongolian poplar (*Populus suaveolens* Fisch.), Siberian spruce (*Picea obovata* Ldb.), and Siberian larch (*Larix sibirica* Ldb.), across this region. The results showed that for the five species, the average biomass proportion for the stems was 75%, followed by branches at 20% and foliage at 5%. The species-specific component and total AGB models for the Khangai region were developed using tree diameter at breast height (D) and D^2 and tree height (H) combined (D^2H); and both D and H were used as independent variables. The best allometric model was $\ln\hat{Y} = \ln a + b \times \ln D + c \times \ln H$ for the various components and total AGB of *B. platyphylla* and *L. sibirica*, for the stems and total AGB of *P. suaveolens*, and for the stem and branch biomass of *P. obovata*. The equation $\ln\hat{Y} = \ln a + b \times \ln(D^2 \times H)$ was best for the various components and total AGB of *P. sibirica*, for the branch and foliage biomass of *P. suaveolens*, and for AGB of *P. obovata*. The equation $\ln\hat{Y} = \ln a + b \times \ln(D)$ was best only for the foliage biomass of *P. obovata*. Our results highlight that developing species-specific tree AGB models is very important for accurately estimating the biomass in the Khangai forest region of Mongolia. Our biomass models will be used at the tree level inventories with sample plots in the Khangai forest region.

Keywords: above-ground biomass; allometric biomass model; biomass allocation; boreal forest; Khangai region; northern Mongolia

1. Introduction

Forest ecosystems play a dual role in global and regional carbon (C) cycles due to their capacity for C storage and high productivity [1,2]. One of the important characteristics of forest ecosystems is biomass, which plays an important role in biogeochemical cycles, ecosystem function and the formation of community structure [3–6]. In the context of global climate change, quantifying and

estimating the above-ground biomass (AGB) and C storage in forest ecosystems using tree biomass models are necessary [7,8]. The estimation of forest ecosystem biomass, including the biomass of tree components, such as stems, branches, foliage, and roots, on local, regional and national scales is essential for determining C storage and forest productivity [9,10]. The biomass and carbon stock changes estimated by the allometric equations are important for assessing the mitigation effect of forests on global climate change, and predicting the potential for C sequestration and emission reduction activities such as tree planting, protecting forests from wildfire and insect or disease outbreak, etc. [11]. Mongolia, as a partner country of the UN-REDD Programme since 2011, is required to submit the national Forest Reference Level to the United Nations Framework Convention on Climate Change (UNFCCC). In the context of climate change and UN-REDD+ activities, biomass productivity and the potential for carbon sequestration have received much more attention than hitherto [8].

Mongolia has 18.5×10^6 hectares of forest land, including 12.3×10^6 hectares of closed (canopy cover more than 20%) and open forests distributed on the southernmost edge of the vast Siberian boreal forest and the northern edge of the Central Asian deserts and most forest in Khangai region is natural forest and rarely disturbed by human beings; these areas exhibit harsh continental climatic conditions. The boreal forest biome represents one of the most important terrestrial C stores, which is an important reason to intensively research C densities in this area [12]. Thus, the forest land of Mongolia can be divided into two different biomes, namely, northern deciduous or coniferous boreal forests (84.7%) and southern saxaul forests (15.3%) [13]. The second largest northern boreal forest ecosystem in Mongolia is located in the Khangai forest vegetation region, which includes a natural forest area of 4 million ha with 516 million m^3 of growing stock. However, this region is vulnerable to climate change and anthropogenic and natural forest disturbance factors. The biomass of these boreal forests have important ecological functions, including regulating the water flow of rivers and streams, protecting the soil from erosion, and sequestering and storing C in forest ecosystems [13–17].

To date, no equations have been empirically established to estimate tree biomass in the Khangai region. A few studies have focused on the assessment of the AGB in *Larix sibirica* Ldb. forests in southern Siberia and north-eastern Mongolia [18]. Additionally, some previous studies developed AGB equations for Siberian larch, Scots pine, and Asian white birch trees in the Khentei region of Mongolia [18–20]. Unfortunately, these studies did not provide any methodical details on the calculations in the biomass analyses. Battulga et al. [21] developed regression models for the stem, branch and foliage biomass of Siberian larch in the Altai Mountains based on data from 18 trees. Based on this database, Dulamsuren et al. [12] added the data of 12 trees from the Khangai Mountains and established more accurate biomass regression equations for Siberian larch. For predicting tree biomass more accurately, it is necessary to increase the number of individual trees for developing the most suitable allometric regression models. Therefore, to accurately estimate the forest ecosystem biomass in the Khangai region and even Mongolia, establishing species-specific biomass equations for the main tree species in this region is urgently needed [12,22].

The boreal forests in the Khangai region comprise coniferous and deciduous trees, including Siberian stone pine—*Pinus sibirica* Du Tour. (1.1% of the total forest area), Asian white birch—*Betula platyphylla* Sukacz. (7.9%), Mongolian poplar—*Populus suaveolens* Fisch. (0.2%), Siberian spruce—*Picea obovata* Ldb. (0.2%) and Siberian larch—*Larix sibirica* Ldb. (90.6%). Therefore, we focused on these five tree species. We collected biomass data from 183 tree samples and measured the AGB and biomass components, including the stem, branch and foliage biomass, in the Khangai region of Mongolia. Our objectives were the following: (1) to develop allometric equations for individual tree species for the various biomass components, including the stems, branches, foliage and the total AGB using typical parameters, i.e., the tree diameter at breast height (D) and tree height (H); and (2) to investigate their allocations, including the biomass proportions of stems, branches and foliage, for the five major tree species in the boreal forests of the Khangai region of northern Mongolia.

2. Materials and Methods

2.1. Study Area

A field study was carried out in the Khangai forest vegetation region of Mongolia (Figure 1). The Khangai region occupies the central part of northern Mongolia (between 47°–51° N and 96°–100° E). The highest peak in the Khangai Mountains is Otgontenger, which reaches 4031 m a.s.l., and medium-elevation mountain ranges such as Tarbagatai (3240 m), Bulnai (2619 m), Khan-Khukhi (1928 m) and Buren (1980 m) are also found in the region. Darkhat's depression (1550 m a.s.l.) located in the northern part of Khangai region is surrounded by mountains. The altitude levels in the territory predominately range between 1800–2000 m a.s.l., but the altitude in the north-eastern part is 1200–1400 m a.s.l. The mean annual temperature is −1.3 to −6.5 °C, the monthly average temperature is −22.2 °C to −32.3 °C in January and 14.6 to 17.3 °C in July, the mean annual precipitation is 220–311 mm, and the mean annual relative humidity is 56%–59% [17,23]. The peculiarities of the continental climate, the orographic situation, and widely spread mountain steppes determine the vegetation distribution patterns in the Khangai region and displace forest vegetation to the cooler and moister northern slopes [24].

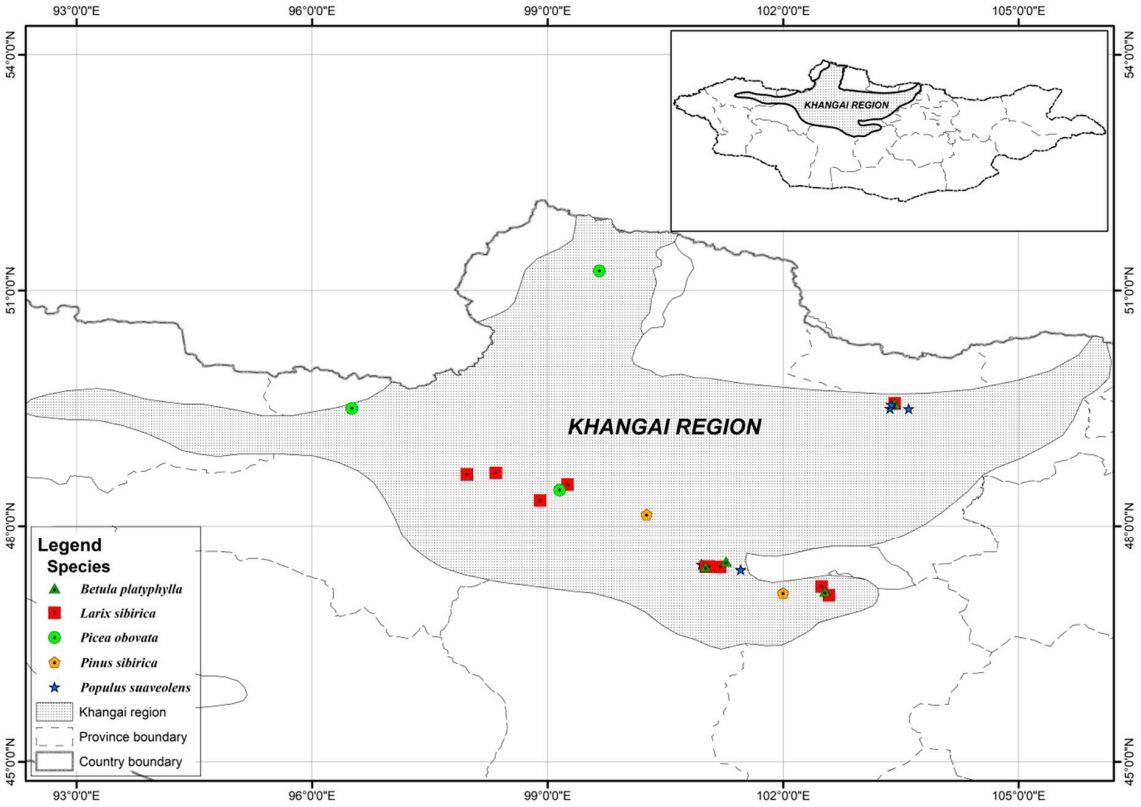

Figure 1. Location of the sample plots in the Khangai region, Mongolia.

2.2. Data Collection

During the field study from 2013 to 2017, a total of 183 sample trees of five species were felled from 26 sample plots and measured in July and August (Figure 1). There were 23 sample trees of Siberian stone pine, 27 sample trees of Asian white birch, 37 sample trees of Mongolian poplar, 22 sample trees of Siberian spruce, and 74 sample trees of Siberian larch (Table 1). The field study was carried out in the most typical forest stands in the Khangai region of Mongolia. A total of 26 circular plots were established, in which there were three plots of *P. sibirica* forest, four plots of *B. platyphylla* forest, five plots of *P. suaveolens* forest, three plots of *P. obovata* forest and 11 plots of *L. sibirica* forest. The radius of

each circular was 20 m. After recording the tree diameters, from 19 sample plots, 5–12 sample trees for each species were selected to be proportional to the number of trees of diameter classes. From four plots, two to three trees representing the mean diameter were selected; also one dominant tree, two intermediate-size trees and one suppressed tree were selected from three sample plots for felling (Table 1). The selected trees were destructively sampled from each plot. The ages of the felled trees were determined by counting the tree rings on the 0.3 m high stumps. The crown of each felled tree was equally divided into top, middle and bottom sections, and all branches in each section were removed from the trunk separately. The stem of each tree was cross-cut at 1–2 m intervals. The fresh weights of the living branches in the crown sections as well as the stems were measured separately using a hanging balance in the field with a precision of ±100 g. A sample branch with an average size was selected from the crown sections, and the branches and foliage were separated and weighed in the field with a precision of ±0.5 g. Sub-samples (50–100 g) from the branches and foliage of each crown section were taken and weighed with a precision of ±0.1 g. At the end of the stem sections, approximately 3 cm-thick discs were cut and weighed. All sub-samples were taken to the laboratory, oven-dried to a constant weight at 105 °C and weighed. The dry biomass of stems, branches, and foliage were computed by multiplying the fresh weight of each component by the dry/fresh weight ratio of corresponding sub-samples. The main characteristics of the sample trees are presented in Table 2.

Table 1. Geographical information describing the location and number of the sampled trees in the Khangai region, Mongolia.

Plot Number	Longitude	Latitude	Elevation (m)	*P. sibirica* (Number)	*B. platyphylla* (Number)	*P. suaveolens* (Number)	*P. obovata* (Number)	*L. sibirica* (Number)
1	98.34	48.68	1993	-	-	-	-	10
2	98.91	48.33	2214	-	-	-	-	3
3	100.96	47.51	1735	-	-	10	-	-
4	102.00	47.14	1453	4	-	-	-	-
5	101.20	47.47	1849	10				
6	100.26	48.15	2195	9	-	-	-	
7	101.20	47.47	1804	-	-	-	-	6
8	101.01	47.48	1683	-	-	-	-	5
9	101.05	47.48	1791	-	-	-	-	2
10	102.49	47.22	1817	-	-	-	-	8
11	102.59	47.11	1933	-	-	-	-	9
12	99.25	48.53	1830	-	-	-	-	9
13	101.01	47.48	1849	-	3	-	-	-
14	101.27	47.54	1771	-	7	-	-	-
15	101.46	47.44	1686	-	-	13	-	-
16	99.66	51.25	1567	-	-	-	4	-
17	96.51	49.50	1890	-	-	-	10	-
18	96.10	49.73	1345	-	-	-	8	-
19	97.97	48.66	2035	-	-	-	-	5
20	97.97	48.66	2033	-	-	-	-	6
21	103.42	49.56	1091	-	-	-	-	11
22	102.53	47.16	1782	-	9	-	-	-
23	103.42	49.56	1101	-	8	-	-	-
24	103.36	49.50	957	-	-	3	-	-
25	103.60	49.50	963	-	-	4	-	-
26	103.38	49.55	868	-	-	7	-	-
Total				23	27	37	22	74

Table 2. Statistical characteristics and biomass of the five tree species.

Species	Value	D (cm)	H (m)	Stem (kg)	Branch (kg)	Foliage (kg)	Total AGB (kg)	Age (years)
P. sibirica	Mean	23.0	11.5	148.71	62.32	12.19	223.22	95
	SD	11.8	4.0	137.52	62.18	11.91	207.7	46
	SE	2.5	0.8	28.68	12.97	2.48	43.31	10
	Min	2.0	2.5	0.476	0.10	0.07	0.80	9
	Max	42.0	17.6	458.10	193.19	42.72	667.74	194
B. platyphylla	Mean	16.4	12.7	98.30	31.87	4.26	134.42	56
	SD	7.4	5.1	114.64	37.33	4.64	151.41	18
	SE	1.4	1.0	22.06	7.18	0.89	29.14	3
	Min	6.0	6.2	4.58	1.26	0.21	6.47	18
	Max	35.4	22.5	491.76	139.51	18.41	602.81	95
P. suaveolens	Mean	25.3	13.6	187.73	68.26	6.93	262.92	61
	SD	15.1	5.2	255.34	95.66	5.92	350.19	25
	SE	2.5	0.9	41.98	15.73	0.97	57.57	4
	Min	5.2	5.1	1.76	0.66	0.22	3.33	18
	Max	68.0	25.5	1311.37	439.89	23.03	1766.87	120
P. obovata	Mean	21.9	16.4	193.53	32.56	16.34	242.43	137
	SD	10.7	6.0	192.00	30.82	12.74	231.78	39
	SE	2.3	1.3	40.94	6.57	2.72	49.42	8
	Min	5.6	5.8	2.76	1.519	1.07	5.35	66
	Max	43.7	27.0	693.34	102.39	52.4	848.14	185
L. sibirica	Mean	23.0	15.5	212.93	37.87	4.83	255.63	88
	SD	12.7	5.9	262.24	45.88	4.94	300.18	56
	SE	1.5	0.7	30.49	5.33	0.58	34.9	6
	Min	3.8	4.3	1.147	0.52	0.05	2.1	27
	Max	52.5	31.4	1104.02	201.81	22.07	1238.66	259

Note: D—diameter at breast height; H—tree height; AGB—above-ground biomass; Mean—arithmetic mean; SD—standard deviation; SE—standard error; Min—minimum value; Max—maximum value.

2.3. Statistical Analysis

Three commonly used allometric models [21,25–27] were tested for estimating each component and the AGB of trees using the diameter at breast height (D in cm) and tree height (H in m):

$$\hat{Y} = aD^b \quad (1)$$

$$\hat{Y} = a(D^2H)^b \quad (2)$$

$$\hat{Y} = aD^b\ H^c \quad (3)$$

where $\hat{Y}$ is the predicted tree biomass value in kg and a, b and c are the fitted parameters.

In forest biomass studies, the error variances for the allometric nonlinear equations based on arithmetical units of measurement are not constant over all observations (heteroscedasticity) in most cases [28]. Using log-transformed data for linear regressions when estimating the parameters in nonlinear models is one of the most commonly used methods for eliminating the influences of heteroscedasticity [7,29–31]. Consequently, Equations (1) to (3) were linearized using logarithms in the following equations:

$$\ln\hat{Y} = \ln a + b \times \ln D \quad (4)$$

$$\ln\hat{Y} = \ln a + b \times \ln(D^2 \times H) \quad (5)$$

$$\ln\hat{Y} = \ln a + b \times \ln D + c \times \ln H \quad (6)$$

where $\ln\hat{Y}$ is the predicted tree biomass value in the logarithmic unit and lna, b and c are the fitted parameters.

Log-transformed linear regression Equations (4) to (6) have commonly been used for modelling above-ground tree biomass in many studies [20,27,32,33]. Models were calculated separately for the

stems, branches, foliage and AGB. The antilog transformation of the predicted logarithmic values to arithmetic units leads to a systematic bias that can generally be corrected with the following correction factor [28,34]:

$$\mathrm{CF} = \exp(\mathrm{RMSE}^2/2) \tag{7}$$

where CF is the correction, RMSE is the root mean square error from the logarithmic regression, and n is the sample size. For selecting the best model for the total biomass and each biomass component of the trees, we used model fitting and performance statistics such as the coefficient of determination (R^2), RMSE, mean absolute bias (MAB), and Akaike information criteria (AICc):

$$R^2 = 1 - \left(\frac{\sum_{i=1}^{n} (\ln Y - \ln \bar{Y})^2}{\sum_{i=1}^{n} \left(\ln Y - \ln \hat{Y} \right)^2} \right) \tag{8}$$

$$\mathrm{RMSE} = \sqrt{\sum_{i=1}^{n} \left(\ln Y - \ln \hat{Y} \right)^2 / (n - p - 1)} \tag{9}$$

$$\mathrm{MAB} = \sum_{1}^{n} \frac{\left(\left| \ln Y - \ln \hat{Y} \right| \right)}{n} \tag{10}$$

$$\mathrm{AICc} = n \log\left(\frac{\mathrm{RSS}}{n} \right) + 2k + \frac{2k(k+1)}{n-k-1} \tag{11}$$

$$\Delta \mathrm{AICc}_i = \mathrm{AICc}_i - \mathrm{AICc}_{min}, \text{ for } i = 1, 2 \ldots R \tag{12}$$

where ln Y is the observed log-transformed biomass value, $\ln \hat{Y}$ is the predicted log-transformed biomass value from the fitted model, n is the sample size, $\ln \bar{Y}$ is the mean of the observed log-transformed biomass value, p is the number of terms in the model, RSS is the residual sum of squares from the fitted model, k is the number of parameters, $\Delta \mathrm{AICc}_i$ is the AICc difference, and $\Delta \mathrm{AICc}_{min}$ is the minimum of the AICc values for the R models. High R^2 values, small RMSE, MAB, and AICc values and a $\Delta \mathrm{AICc}_i = 0$ indicate high model precision.

Considering our small sample size, we used the leave-one-out method to cross-validate our best equations [35,36].

3. Results

3.1. AGB of Tree Species and Biomass Partitioning

The total AGB was highest in *P. suaveolens* (263 ± 43 kg), followed by *L. sibirica* (256 ± 35 kg), *P. obovata* (242 ± 49 kg), *P. sibirica* (223 ± 43 kg) and *B. platyphylla* (134 ± 29 kg) in the Khangai region (Table 2). The average biomass proportion in the stems was 75%, followed by 20% in the branches and 5% in the foliage when the five tree species were combined (Table 3). The partitioning of total tree AGB into the biomass of the tree components for the five species across diameter classes is shown in Figure 2. The results indicated that the biomass proportion was largest in the stems for each of the five species (64%–88%), but the trend was not the same for each species. For *P. sibirica*, the relative contribution of stem biomass to the total AGB increased from 66% for the small-diameter class (<10 cm) to 76% for the medium-diameter class (10–20 cm); however, the relative contribution decreased slightly to 65% for the large-diameter classes (30–40 cm) due to the extensively higher relative contribution of branch biomass to the total AGB. For *P. suaveolens*, *L. Sibirica*, *P. obovata*, *B. platyphylla* and the five species combined, the relative contribution of stem biomass to the total AGB increased with increasing tree diameter classes. In general, the relative contribution of branch biomass to the total AGB increased with increasing diameter classes for *P. sibirica, B. platyphylla, P. suaveolens and* the five species combined; however, the relative contribution decreased for *L. sibirica* and *P. obovata*. For all five tree species,

the relative contribution of foliage biomass to the total AGB decreased with increasing tree diameter class (Figure 2).

Table 3. Ratio of the stem, branch and foliage biomass to the total above-ground biomass of the sample trees.

Species	Stem Biomass/AGB			Branch Biomass/AGB			Foliage Biomass/AGB		
	Mean	SD	Range	Mean	SD	Range	Mean	SD	Range
P. sibirica	0.68	0.07	0.55–0.87	0.25	0.07	0.07–0.37	0.07	0.05	0.03–0.28
B. platyphylla	0.73	0.09	0.52–0.90	0.23	0.08	0.08–0.42	0.04	0.02	0.00–0.10
P. suaveolens	0.70	0.10	0.50–0.87	0.26	0.08	0.10–0.40	0.05	0.03	0.01–0.13
P. obovata	0.76	0.09	0.51–0.86	0.15	0.06	0.08–0.28	0.09	0.05	0.05–0.21
L. sibirica	0.81	0.10	0.54–0.93	0.16	0.09	0.05–0.36	0.03	0.02	0.00–0.09
Total	0.75	0.11	0.50–0.94	0.20	0.09	0.05–0.42	0.05	0.04	0.00–0.28

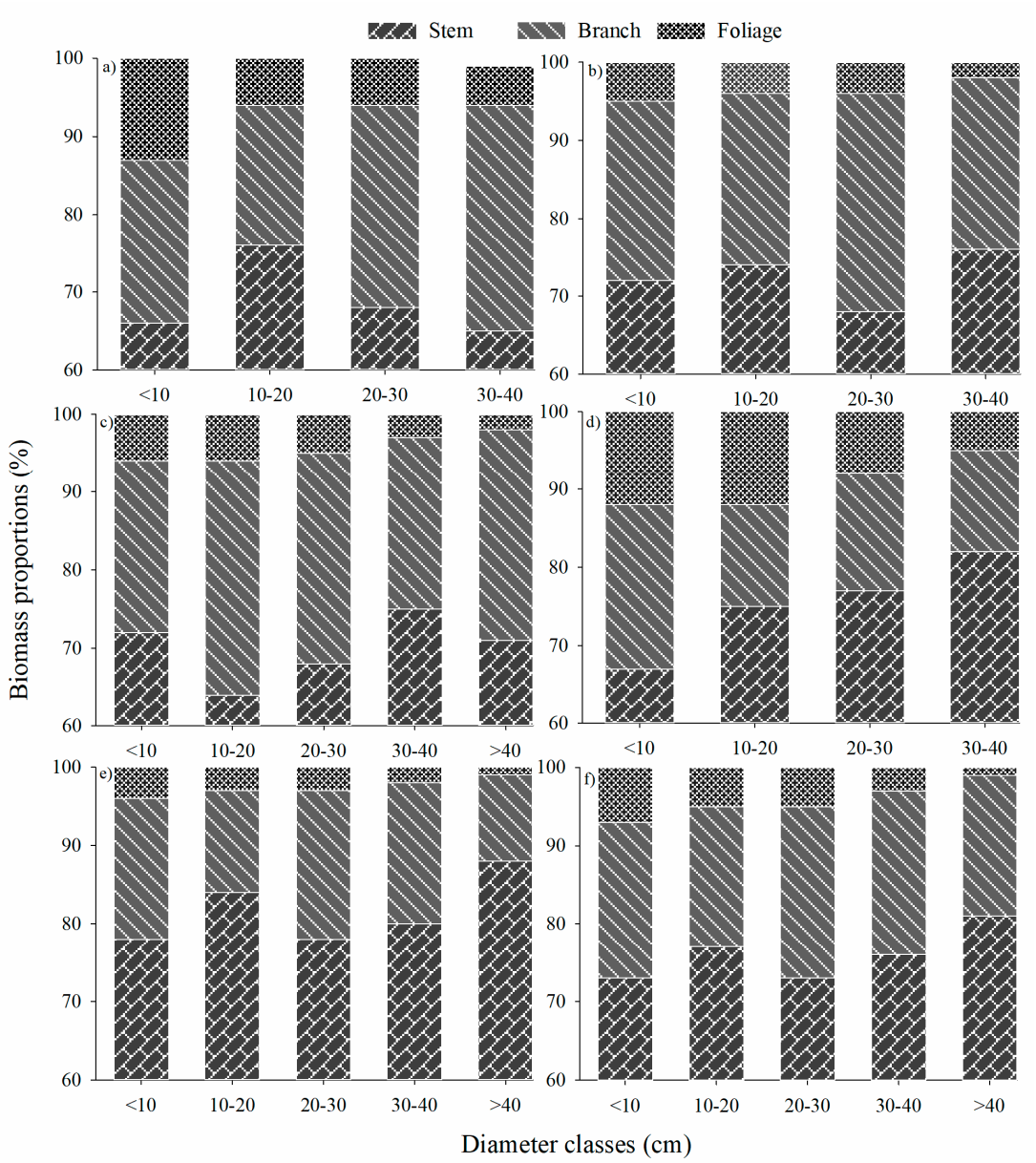

Figure 2. Biomass partitioning of the above-ground components across the 10 cm diameter classes. (**a**) *Pinus sibirica*, (**b**) *Betula platyphylla*, (**c**) *Populus suaveolens*, (**d**) *Picea obovata*, (**e**) *Larix sibirica* and (**f**) the five species combined.

3.2. Allometric Biomass Equations

In this study, we tested three candidate log-transformed allometric equations (Equations (4)–(6)) to develop the best and most accurate allometric models for estimating the foliage, branch, and stem biomass and the total AGB for the five tree species. The results of the regression analysis and analysis of variance of the fitted equations and validation statistics are presented in Table 4. In addition, the analysis of multicollinearity for Equation (6) and residual analysis for all equations were did and the results were showed for all the best equations (Table S2 and Figure S2). All regression equations had good fits ($p < 0.001$). The models with high R^2 values, low MAB, RMSE, and AICc values and ΔAICc differences were used to choose the best-fit models. If the difference between the MAB and RMSE values and the difference between the AICc scores of the compared equations were insignificant and differed slightly more or less, then the equation with a higher R^2 value was selected (Table 4). Therefore, the best performing and accurate allometric models that were found differed among the different species and different components. For example, the equation $\ln\hat{Y} = \ln a + b \times \ln D + c \times \ln H$ was selected as the best model for each component and the total tree AGB of *B. platyphylla* and *L. sibirica*, for the stem biomass of *P. suaveolens* and *P. obovata*, and for the branch biomass of *P. obovata*. The equation $\ln\hat{Y} = \ln a + b \times \ln(D^2 \times H)$ was selected for each component and the total tree AGB of *P. sibirica* and for the branch and foliage biomass of *P. suaveolens*. The equation $\ln\hat{Y} = \ln a + b \times \ln(D)$ was selected only for the foliage biomass of *P. obovata* (Table 4). All of the "best equations" showed a significant and robust fitting effect for predicting a given component biomass or total AGB. The mean R^2 values for the fitted biomass of foliage and branches were 0.83 and 0.93, respectively, and those for the stems and total AGB were 0.99 and 0.98, respectively. The combined variables of D and H explained more than 80.0% of the variation in most of the biomass components, except for the foliage biomass (74.7%) of *B. platyphylla* (Table 4).

The cross-validation for our best equations, using the leave-one-out method, showed that the stem, branch and total AGB best equations were robust, although the R^2 values for foliage equations were lower, the validation results were significant which indicated that the best equations were reliable and could be used in the investigation of forest biomass stocks and changes in Khangai region, Mongolia (Table S3, Figure S3).

Table 4. Parameter estimates and model evaluation statistics of each model for the stem, branch, foliage, and above-ground biomass for the five tree species in the Khangai region, Mongolia.

Component	Equation *	lna	b	c	R^2	RMSE	MAB	AICc	ΔAIC	CF
				P. sibirica						
	$\ln\hat{Y} = \ln a + b \times \ln D$	−2.606	2.314	-	0.988	0.198	0.164	−69.300	7.900	1.020
Stem	**$\ln\hat{Y} = \ln a + b \times \ln(D^2 \times H)$**	−3.128	0.889	-	**0.992**	**0.167**	0.125	**−77.200**	**0.000**	1.014
	$\ln\hat{Y} = \ln a + b \times \ln D + c \times \ln H$	−3.214	1.685	1.042	0.992	0.170	**0.123**	−38.000	39.200	1.015
	$\ln\hat{Y} = \ln a + b \times \ln D$	−4.376	2.554	-	0.952	0.446	0.305	−31.900	0.100	1.105
Branch	**$\ln\hat{Y} = \ln a + b \times \ln(D^2 \times H)$**	−4.939	0.980	-	0.952	**0.446**	0.310	**−32.000**	**0.000**	1.104
	$\ln\hat{Y} = \ln a + b \times \ln D + c \times \ln H$	−4.672	2.247	0.507	**0.953**	0.454	**0.306**	−29.300	2.700	1.109
	$\ln\hat{Y} = \ln a + b \times \ln D$	−3.950	1.946	-	0.850	0.637	0.470	−15.600	0.700	1.225
Foliage	**$\ln\hat{Y} = \ln a + b \times \ln(D^2 \times H)$**	−4.395	0.748	-	**0.855**	**0.627**	0.458	**−16.300**	**0.000**	1.217
	$\ln\hat{Y} = \ln a + b \times \ln D + c \times \ln H$	−4.629	1.243	1.163	0.855	0.641	**0.453**	−13.500	2.800	1.228
	$\ln\hat{Y} = \ln a + b \times \ln D$	−2.219	2.315	-	0.984	0.226	0.177	−63.200	3.100	1.026
Total AGB	**$\ln\hat{Y} = \ln a + b \times \ln(D^2 \times H)$**	−2.736	0.889	-	0.986	**0.211**	**0.160**	**−66.300**	**0.000**	1.025
	$\ln\hat{Y} = \ln a + b \times \ln D + c \times \ln H$	−2.680	1.839	0.788	**0.987**	0.216	0.160	−63.400	2.900	1.024
				B. platyphylla						
	$\ln\hat{Y} = \ln a + b \times \ln D$	−3.031	2.591	-	0.974	0.209	0.159	−79.600	32.000	1.022
Stem	$\ln\hat{Y} = \ln a + b \times \ln(D^2 \times H)$	−3.618	0.964	-	0.992	0.119	0.088	−110.200	1.400	1.007
	$\ln\hat{Y} = \ln a + b \times \ln D + c \times \ln H$	−3.535	2.073	0.771	**0.993**	**0.112**	**0.080**	**−111.600**	**0.000**	1.006
	$\ln\hat{Y} = \ln a + b \times \ln D$	−4.298	2.619	-	0.908	0.411	0.319	−43.100	1.600	1.088
Branch	$\ln\hat{Y} = \ln a + b \times \ln(D^2 \times H)$	−4.546	0.930	-	0.842	0.536	0.414	−28.700	16.000	1.155
	$\ln\hat{Y} = \ln a + b \times \ln D + c \times \ln H$	−3.845	3.085	−0.693	**0.921**	**0.386**	**0.285**	**−44.800**	**0.000**	1.077
	$\ln\hat{Y} = \ln a + b \times \ln D$	−4.794	2.105	-	0.733	0.624	0.460	**−20.500**	**0.000**	1.215
Foliage	$\ln\hat{Y} = \ln a + b \times \ln(D^2 \times H)$	−4.978	0.746	-	0.677	0.686	0.535	−15.400	5.100	1.265
	$\ln\hat{Y} = \ln a + b \times \ln D + c \times \ln H$	−4.389	2.522	−0.621	**0.747**	**0.620**	**0.443**	−19.200	1.300	1.212
	$\ln\hat{Y} = \ln a + b \times \ln D$	−2.674	2.580	-	0.986	0.154	0.126	−96.200	10.600	1.012
Total AGB	$\ln\hat{Y} = \ln a + b \times \ln(D^2 \times H)$	−3.176	0.949	-	0.982	0.173	0.127	−89.900	16.900	1.015
	$\ln\hat{Y} = \ln a + b \times \ln D + c \times \ln H$	−2.947	2.299	0.417	**0.991**	**0.122**	**0.088**	**−106.800**	**0.000**	1.008
				P. suaveolens						
	$\ln\hat{Y} = \ln a + b \times \ln D$	−2.895	2.369	-	0.981	0.220	0.147	−106.400	17.800	1.026
Stem	$\ln\hat{Y} = \ln a + b \times \ln(D^2 \times H)$	−3.630	0.921	-	0.988	**0.175**	0.111	**−124.200**	**0.000**	1.016
	$\ln\hat{Y} = \ln a + b \times \ln D + c \times \ln H$	−3.792	1.717	1.136	**0.989**	0.176	**0.109**	−122.500	1.700	1.016

Table 4. *Cont.*

Component	Equation *	lna	b	c	R^2	RMSE	MAB	AICc	ΔAIC	CF
	$\ln\hat{Y} = \ln a + b \times \ln D$	−3.949	2.380	-	0.935	0.430	0.320	−57.800	0.800	1.109
Branch	**$\ln\hat{Y} = \ln a + b \times \ln(D^2 \times H)$**	−4.665	0.923	-	**0.936**	**0.426**	0.320	**−58.500**	**0.000**	1.108
	$\ln\hat{Y} = \ln a + b \times \ln D + c \times \ln H$	−4.419	2.039	0.595	0.936	0.429	**0.319**	−56.400	2.200	1.110
	$\ln\hat{Y} = \ln a + b \times \ln D$	−3.870	1.745	-	0.809	0.580	0.447	−35.700	0.300	1.205
Foliage	**$\ln\hat{Y} = \ln a + b \times \ln(D^2 \times H)$**	−4.395	0.677	-	**0.810**	**0.580**	0.450	**−35.900**	**0.000**	1.210
	$\ln\hat{Y} = \ln a + b \times \ln D + c \times \ln H$	−4.226	1.486	0.451	0.810	0.585	**0.448**	−33.500	2.400	1.212
	$\ln\hat{Y} = \ln a + b \times \ln D$	−1.929	2.194	-	0.937	0.390	0.215	**−65.600**	**0.000**	1.022
Total AGB	$\ln\hat{Y} = \ln a + b \times \ln(D^2 \times H)$	−2.558	0.847	-	0.931	0.406	0.225	−62.000	3.600	1.016
	$\ln\hat{Y} = \ln a + b \times \ln D + c \times \ln H$	−1.795	2.291	−0.170	**0.938**	**0.390**	**0.214**	−64.200	2.400	1.016
				P. obovata						
	$\ln\hat{Y} = \ln a + b \times \ln D$	−3.104	2.590	-	0.971	0.260	0.196	−54.000	11.500	1.034
Stem	$\ln\hat{Y} = \ln a + b \times \ln(D^2 \times H)$	−3.732	0.959	-	0.983	0.200	0.153	**−65.500**	**0.000**	1.020
	$\ln\hat{Y} = \ln a + b \times \ln D + c \times \ln H$	−4.064	1.507	1.526	**0.985**	**0.194**	**0.153**	−65.000	0.400	1.019
	$\ln\hat{Y} = \ln a + b \times \ln D$	−3.741	2.239	-	0.937	**0.335**	0.261	**−42.800**	**0.000**	1.058
Branch	$\ln\hat{Y} = \ln a + b \times \ln(D^2 \times H)$	−4.202	0.819	-	0.927	0.362	0.279	−39.500	3.300	1.068
	$\ln\hat{Y} = \ln a + b \times \ln D + c \times \ln H$	−3.484	2.528	−0.409	**0.939**	0.340	**0.256**	−40.300	2.600	1.060
	$\ln\hat{Y} = \ln a + b \times \ln D$	−3.287	1.910	-	0.912	**0.345**	**0.278**	**−41.600**	**0.000**	1.061
Foliage	$\ln\hat{Y} = \ln a + b \times \ln(D^2 \times H)$	−3.712	0.703	-	0.911	0.346	0.293	−41.500	0.100	1.062
	$\ln\hat{Y} = \ln a + b \times \ln D + c \times \ln H$	−3.490	1.681	0.323	**0.913**	0.351	0.284	−38.800	2.800	1.064
	$\ln\hat{Y} = \ln a + b \times \ln D$	−2.419	2.455	-	0.980	0.204	0.144	**−75.200**	**0.000**	1.021
Total AGB	**$\ln\hat{Y} = \ln a + b \times \ln(D^2 \times H)$**	−2.994	0.907	-	**0.987**	**0.165**	**0.123**	−74.000	1.200	1.014
	$\ln\hat{Y} = \ln a + b \times \ln D + c \times \ln H$	−3.063	1.727	1.025	0.987	0.169	0.124	−71.100	4.100	1.014
				L. sibirica						
	$\ln\hat{Y} = \ln a + b \times \ln D$	−2.858	2.471	-	0.975	0.244	0.203	−205.200	66.100	1.030
Stem	$\ln\hat{Y} = \ln a + b \times \ln(D^2 \times H)$	−3.738	0.955	-	0.990	0.155	0.124	**−271.300**	**0.000**	1.012
	$\ln\hat{Y} = \ln a + b \times \ln D + c \times \ln H$	−3.818	1.849	1.053	**0.990**	**0.155**	**0.123**	−270.000	1.300	1.012
	$\ln\hat{Y} = \ln a + b \times \ln D$	−4.404	2.393	-	0.866	0.580	0.464	−76.300	14.700	1.183
Branch	$\ln\hat{Y} = \ln a + b \times \ln(D^2 \times H)$	−4.993	0.894	-	0.822	0.669	0.540	−55.200	35.800	1.251
	$\ln\hat{Y} = \ln a + b \times \ln D + c \times \ln H$	−3.060	3.263	−1.474	**0.894**	**0.521**	**0.402**	**−91.000**	**0.000**	1.145
	$\ln\hat{Y} = \ln a + b \times \ln D$	−4.900	1.960	-	0.797	0.610	0.483	**−93.200**	**0.000**	1.204
Foliage	$\ln\hat{Y} = \ln a + b \times \ln(D^2 \times H)$	−5.371	0.731	-	0.754	0.672	0.522	−68.900	24.400	1.253
	$\ln\hat{Y} = \ln a + b \times \ln D + c \times \ln H$	−3.701	2.736	−1.315	**0.827**	**0.567**	**0.440**	−52.300	40.900	1.174
	$\ln\hat{Y} = \ln a + b \times \ln D$	−2.544	2.437	-	0.982	0.204	0.166	−80.700	167.000	1.021
Total AGB	$\ln\hat{Y} = \ln a + b \times \ln(D^2 \times H)$	−3.361	0.936	-	0.984	0.192	0.153	−230.800	17.300	1.019
	$\ln\hat{Y} = \ln a + b \times \ln D + c \times \ln H$	−3.048	2.111	0.552	**0.986**	**0.180**	**0.144**	**−248.200**	**0.000**	1.016

Note: * indicates that the p value for all allometric equations is <0.001; lna, b and c are the fitted parameters; R^2 is the coefficient of determination; RMSE is root mean square error; MAB is mean absolute bias; AICc is Akaike information criterion; ΔAIC is the minimum of the AICc values; and CF is correction factor. The statistical values pivotal for the selection of the relevant regression model, which is more suitable for biomass prediction, are printed in bold.

4. Discussion

4.1. Biomass Partitioning

DBH is a representative indicator of biomass allocation, and trees with different DBH sizes have different biomass allocation strategies [37]. In this study, the DBH for all of the tree samples was divided into five classes: <10 cm, 10–20 cm, 20–30 cm, 30–40 cm and >40 cm. The results showed that the proportion of foliage biomass decreased gradually with increasing basal diameter, which indicates that relatively more biomass was allocated to the trunk and roots to absorb nutrients for improved growth. This result was consistent with previous studies [10,25,31]. Nevertheless, the proportions of stem and branch biomass did not show a clear trend for the five tree species. This finding may be because the DBH of the trees was not large enough to show certain regularity. However, Vargas-Larreta et al. [38] found that the proportion of stem biomass in pine trees increased with diameter, although the proportion of foliage biomass decreased and was fairly stable for the branch biomass. Similarly, in the current study, the relative contribution of foliage biomass to the total AGB decreased for all five species as the tree stem diameter increased, which was consistent with recent previous studies [10,26,38]. Additionally, we also found that the proportion of stem biomass increased gradually with increasing tree age, while the proportions of branch and foliage biomass decreased with increasing age (Figure S1), which is consistent with many previous studies [27,39–42]. These findings suggest that more biomass will be allocated to the stems in old trees, which allows the trees to immobilize themselves better and transport more water and nutrients into photosynthetic components.

4.2. Biomass Equation

Many studies have focused on typical allometric equations based on power function models to improve biomass estimations. In this study, we chose three allometric equations as candidates to estimate the biomass equations. The equation with one variable, $\hat{Y} = aD^b$ (1), provides reasonably accurate biomass predictions for many species, sites and regions [7,19,29,43], but the inclusion of tree height in single diameter allometric models results in more accurate biomass predictions [25,26,43–47]. The equation $\hat{Y} = a(D^2H)^b$ (2) improved the model fit for the total AGB and stem and root biomass [44,45] and for all biomass components of some species and the AGB [38]. The equation $\hat{Y} = aD^bH^c$ (3) was the most suitable for predicting the stem volume and biomass [25] and needle biomass for all tree species [21]. In the current study, species-specific component and total AGB log-transformed models for the Khangai region were developed using tree diameter at breast height (D), D^2 and height combined (D^2H), and both D and H were independent variables. The log-transformation of real data resulted in the homoscedasticity of the dependent variable, AGB [48]. The results of our study on the development of tree components and total AGB were consistent with many of the aforementioned previous studies. We compared our best stem biomass equations for *L. sibirica* and *B. platyphylla* in the Khangai region with the stem biomass equations published by Battulga et al. [21] for Altai Mountain, Dulamsuren et al. [12] for a forest-steppe in Mongolia, Usoltsev et al. [49] for Eurasia and Dong et al. [26] for China. Figure 3 shows that the line of our equation is the closest to the line (1:1) of the measured stem biomass. The comparison between our best equation with the equations from previous studies for the estimation of the stem biomass of *L. Sibirica* showed that the equation from Battulga et al. [21] underestimated stem biomass, and the equations from Dulamsuren et al. [12] and Usoltsev et al. [49] overestimated stem biomass (Figure 3). Additionally, the comparison for the estimation of the stem biomass of *B. platyphylla* showed that the stem biomass equation from Dong et al. [26] underestimated stem biomass, while the equation from Usoltsev et al. [49] overestimated stem biomass (Figure 3). Consequently, we can assume that our equations successfully predicted the stem biomass in this region.

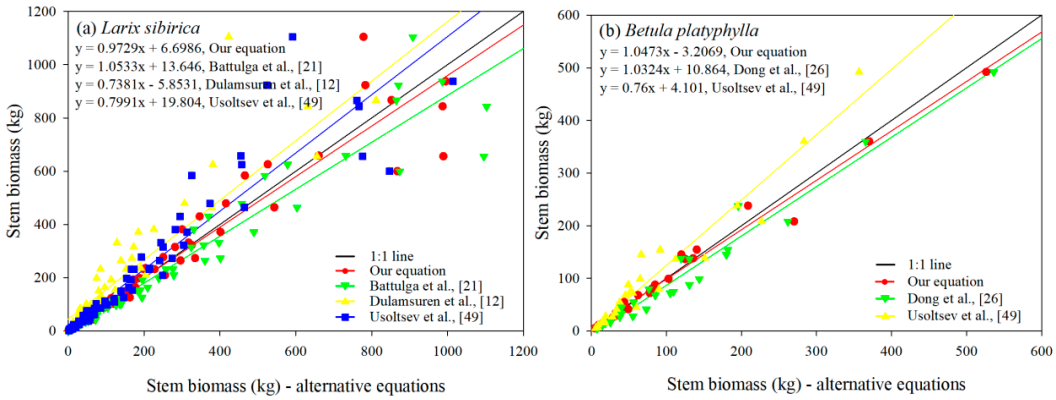

Figure 3. Comparison of allometric functions to estimate stem biomass (kg). The 1:1 line is plotted from measured biomass. (**a**) For the comparison of *L. sibirica*, circles represent the linear function from our equation; inverted triangles represent the linear function from Battulga et al. [21]; triangles represent the linear function from Dulamsuren et al. [12]; and squares represent the linear function from Usoltsev et al. [49]. (**b**) For the comparison of *B. platyphylla*, circles represent the linear function from our equation; inverted triangles represent the linear function from Dong et al. [26], and triangles represent the linear function from Usoltsev et al. [49].

In many studies, four tree components (e.g., stems, roots, branches, and foliage) are involved in development. The sum of biomass predictions from separate tree component models may not equal the biomass prediction of the total tree biomass model [50,51]. To eliminate this inconsistency, several model specifications and estimation methods have been suggested for forcing additivity on a series of biomass equations, both linear and nonlinear [45,51–55]. The property of additivity assures regression functions that are consistent with one other. That is, if the biomass of one tree component is part of the total tree biomass, it is logical to expect the estimate of the part not to exceed the estimate of the total tree biomass [51]. Consequently, we examined the consistency between the total AGB calculated as the sum of the best models for the above-ground component biomass with stems, branches and foliage, $y = y_{stem} + y_{branch} + y_{foliage}$ (procedure 1 in Parresol [51]), and predicted the total tree AGB of the best models for each of the five tree species (Figure 4). The Wilcoxon rank sum test was used due to the non-normality of those data. The results showed that the predicted total tree AGB of the best models (Estimation 1) and the AGB calculated as the sum of the best models for the above-ground component biomass (Estimation 2) differed slightly (Figure 4). For the statistical population of sample trees, the mean differences between the total tree AGBs calculated by the best models and the sum of the best models for the above-ground component biomass for each species were very small (from 0.3 kg to 3.1 kg, but 16.9 kg for *P. suaveolens*), and the p values were 0.91–0.99 (Table S1). Thus, the differences in means were not statistically significant. Additionally, the differences between the total tree AGB measured and calculated by the best models for the total AGB and the sum of the component biomass were not statistically significant (minimum p values 0.889 > 0.05), indicating that all best models for the total tree AGB and the sum of the component biomass can be used in forest inventory practices. However, the total AGB calculated by the sum of the component biomass models (procedure 1 in Parresol [51]) was slightly better. However, it is necessary that the sum of the best above-ground component biomass models equal the total in the AGB models. For this purpose, we suggest a one-step proportional weighting system for AGB based on a disaggregated model structure (namely, a two-step proportional weighting system, the TSEM method) proposed by Tang et al. [52]; this structure was successfully interpreted as a three-step proportional weighting system, the 3SPW method, and has been implemented in China [54] and Russia [55]. Using the disaggregation method, the total tree predicted AGB, $\hat{Y}_a$, stem (wood + bark) biomass, $f_s(X)$, branch biomass, $f_b(X)$, and foliage biomass, $f_f(X)$, are separately fitted, and the best models are selected. The sum of these component models

must be estimated. The estimated total tree AGB, $\hat{Y}_a$, is proportionally divided into estimates of stem biomass, $\hat{Y}_s$, branch biomass, $\hat{Y}_b$ and foliage biomass, $\hat{Y}_f$, as follows:

$$\hat{Y}_s = \frac{f_s(X)}{f_s(X) + f_b(X) + f_f(X)} \times \hat{Y}_a \quad (13)$$

$$\hat{Y}_b = \frac{f_b(X)}{f_s(X) + f_b(X) + f_f(X)} \times \hat{Y}_a \quad (14)$$

$$\hat{Y}_f = \frac{f_f(X)}{f_s(X) + f_b(X) + f_f(X)} \times \hat{Y}_a \quad (15)$$

The one-step proportional weighting system proved to be good for ensuring the additive property of nonlinear biomass model systems (Table 5).

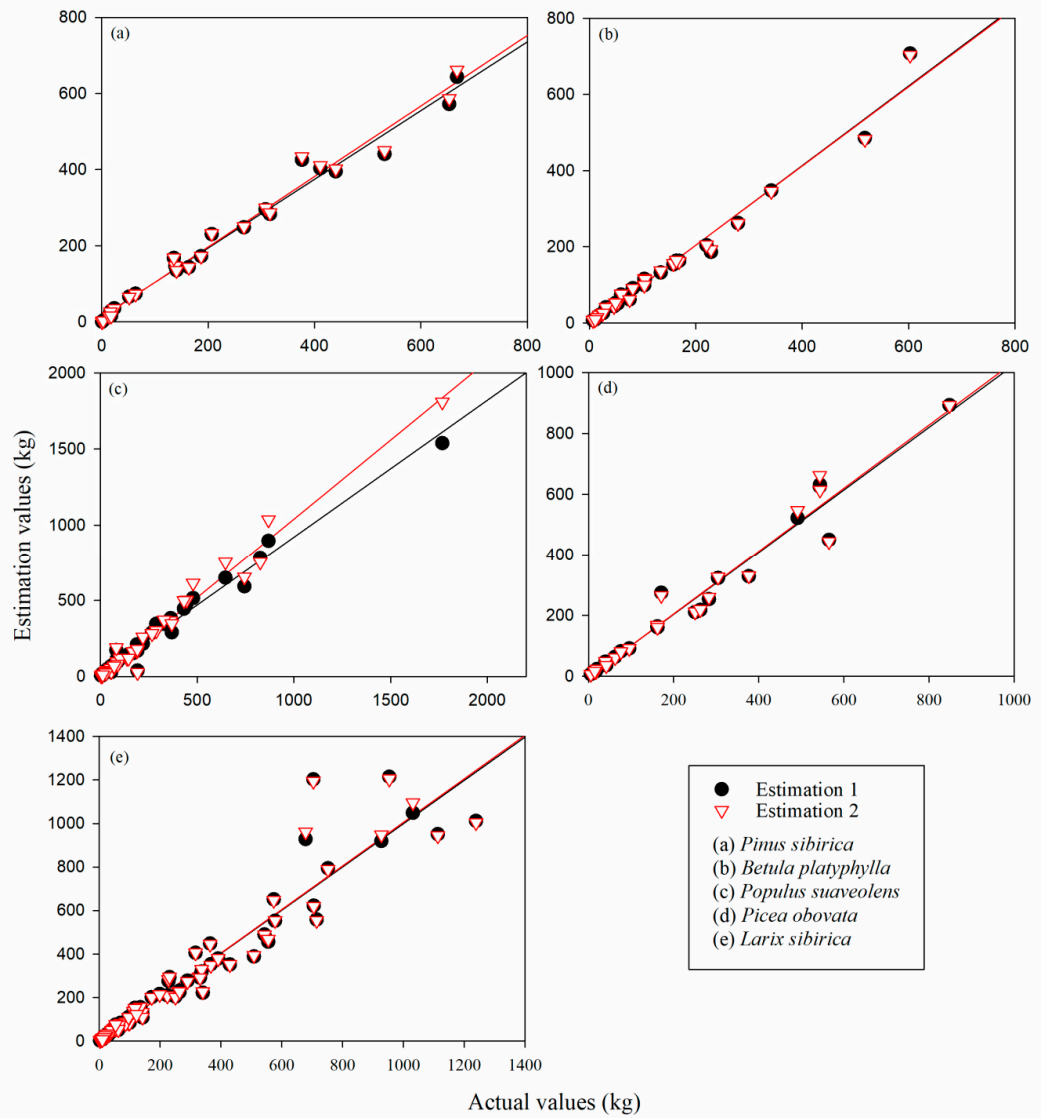

Figure 4. Comparison between the predicted total tree AGB of the best models (Estimation 1) and the AGB calculated as the sum of the best models for the above-ground component biomass (Estimation 2). (**a**) *Pinus sibirica*, (**b**) *Betula platyphylla*, (**c**) *Populus suaveolens*, (**d**) *Picea obovata* and (**e**) *Larix sibirica*.

Table 5. The results of a one-step proportional weighting of the predicted component biomass and total AGB for *Pinus sibirica* Du Tour. from Khangai region, Mongolia.

Items	Predicted Stem BM	Predicted Branch BM	Predicted Needle BM	Sum of Predicted BM	AGB Predicted by Equation (6)	Difference Between 5 and 6
1	2	3	4	5	6	7
Mean component AGB	144.3	61.0	12.8	218.1	215.0	3.1
Weighted mean component AGB	142.3	60.0	12.6	215.0	215.0	0.0

Note: AGB—above-ground biomass of 23 sample trees, kg. BM—biomass, kg. Weighted mean component AGB were calculated by Equations (13) to (15).

4.3. Applied Evaluation

In this study, equations for three components and the total AGB for the five major tree species in the Khangai forest region of Mongolia were established for the first time using tree-level inventories data of this region. As discussed previously, the application of the equations in this study to the same species in other areas will lead to deviations in biomass estimates. Therefore, the application of the biomass equation in this study has certain regional limitations. In addition, within the range of D and H measured in this study, the biomass equation fits achieved good results, and the fitting effect of biomass beyond the range of the D and tree height measured in this study needs further verification.

5. Conclusions

In this study, we examined AGB allocation, including the stem, branch and foliage biomass proportions, for five tree species in boreal forests and developed allometric species-specific component and total AGB models for the Khangai forest region of northern Mongolia. The largest biomass proportion of all five species combined was in the stems (75%), followed by the branches (20%) and foliage (5%). The equation based only on D proved to be best for predicting the foliage biomass of *P. obovata*. Including H as an additional predictor in the equation as D^2H improved the component and total AGB for *P. sibirica* and the branch and foliage biomass for *P. suaveolens*. The equation with both the D and H as predictors significantly improved the predictions of the component and total AGB for *B. platyphylla* and *L. sibirica* as well as the predictions of the stem and branch biomass for some species. Our results highlight that developing species-specific component and total AGB models was very useful for providing significant and accurate estimations of forest biomass in the Khangai region of northern Mongolia.

Supplementary Materials: The following are available online at http://www.mdpi.com/1999-4907/10/8/661/s1, Table S1: The best biomass models and differences between the total tree AGB calculated by the best models and the sum of the best models for the above-ground component biomasses for each species. Table S2: Checking the multicollinearity use the variance inflation factor method for the models estimated with Equation (6). Table S3: The result of leave-one-out validation method. Figure S1: The difference in biomass proportion among the different age groups of trees. One: 0–20 years, two: 20–50 years, three: 50–100 years, four: 100–200 years, and five: more than 200 years. Figure S2: The relationship between residuals with fitted biomass, for a to d is for species: Pinus sibirica; for e to h is for species: Betula platyphyllca; for i to l is for species: Populus suaveolens; for m to p is for species: Picea obovata; for q to t is for species: Larix sibirica. Figure S3: The relationship between actual value and predicted value which were counted by leave-one-out method.

Author Contributions: Conceptualization, H.H. and C.D.; data collection: B.A. (Batbaatar Altanzagas), C.D. and B.A. (Batbaatar Altansukh); methodology: B.A. (Batbaatar Altanzagas), Y.L., C.D., J.F. and H.H.; formal analysis: B.A. (Batbaatar Altanzagas), Y.L. and H.H.; writing—original draft preparation: B.A. (Batbaatar Altanzagas) and Y.L.; writing—review and editing: B.A. (Batbaatar Altanzagas), Y.L., C.D., J.F. and H.H.; supervision: C.D., J.F. and H.H.; All authors contributed critically to the drafts and gave final approval for publication.

Funding: This work has been supported by the Science and Technological Foundation of Mongolia (SST_019/2015), Program–Biodiversity and Adaptation of Key Forest Ecosystems to Climate Change (GIZ) "REDD+ National Forest Inventory in Mongolia" (2013–2017) and the CAS-TWAS President's Fellowship (Batbaatar Altanzagas).

Acknowledgments: We would like to thank the Forest Phytocenology Laboratory, Institute of General and Experimental Biology MAS for assistance in field data collection and the Joint Mongolian and Russian Complex Biological Expedition MAS and RAS for providing vehicles for field research. We are also grateful to the colleague of the Vegetation structure and function group of the State Key Laboratory of Vegetation and Environmental Change, IBCAS, and Enkhmaa Erdenebileg for their comments on the original manuscript.

Conflicts of Interest: The authors declare no conflict of interest.

References

1. Pan, Y.; Birdsey, R.A.; Fang, J.; Houghton, R.; Kauppi, P.E.; Kurz, W.A.; Phillips, O.L.; Shvidenko, A.; Lewis, S.L.; Canadell, J.G.; et al. A large and persistent carbon sink in the world's forests. *Science* **2011**, *333*, 988–993. [CrossRef] [PubMed]
2. Fang, J.; Guo, Z.; Hu, H.; Kato, T.; Muraoka, H.; Son, Y. Forest biomass carbon sinks in East Asia, with special reference to the relative contributions of forest expansion and forest growth. *Glob. Chang. Biol.* **2014**, *20*, 2019–2030. [CrossRef] [PubMed]
3. Kimmins, J.P. *Forest Ecology: A Foundation for Sustainable Forest Management and Environmental Ethics in Forestry*, 3rd ed.; Macmillan: New York, NY, USA, 2003; p. 542.
4. Konôpka, B.; Pajtík, J.; Noguchi, K.; Lukac, M. Replacing Norway spruce with European beech: A comparison of biomass and net primary production patterns in young stands. *For. Ecol. Manag.* **2003**, *302*, 185–192. [CrossRef]
5. Houghton, R. Aboveground forest biomass and the global carbon balance. *Glob. Chang. Biol.* **2005**, *11*, 945–958. [CrossRef]
6. Chen, D.; Huang, X.; Zhang, S.; Sun, X. Biomass modelling of larch (*Larix* spp.) plantations in China based on the mixed model, dummy variable model, and Bayesian hierarchical model. *Forests* **2017**, *8*, 268. [CrossRef]
7. He, H.; Zhang, C.; Zhao, X.; Fousseni, F.; Wang, J.; Dai, H.; Yang, S.; Zuo, Q. Allometric biomass equations for 12 tree species in coniferous and broadleaved mixed forests, Northeastern China. *PLoS ONE* **2018**, *13*, 1–16. [CrossRef]
8. Zeng, W.S. Developing One-variable Individual Tree Biomass Models based on Wood Density for 34 Tree Species in China. *For. Res.* **2018**, *7*, 1–5.
9. Zhang, X.; Cao, Q.V.; Xiang, C.; Duan, A.; Zhang, J. Predicting total and component biomass of Chinese fir using a forecast combination method. *IForest* **2017**, *10*, 687–691. [CrossRef]
10. Dong, L.; Zhang, L.; Li, F. Additive Biomass Equations Based on Different Dendrometric Variables for Two Dominant Species (*Larix gmelini* Rupr. and *Betula platyphylla* Suk.) in Natural Forests in the Eastern Daxing' an Mountains, Northeast China. *Forests* **2018**, *9*, 261. [CrossRef]
11. Picard, N.; Henry, M.; Trotta, C.; Saint-andre, L. Using Bayesian Model Averaging to Predict Tree Aboveground Biomass in Tropical Moist Forests. *For. Sci.* **2012**, *58*, 15–23. [CrossRef]
12. Dulamsuren, C.; Klinge, M.; Degener, J.; Khishigjargal, M.; Chenlemuge, T.; Bat-Enerel, B.; Yeruult, Y.; Sain-Dondov, D.; Ganbaatar, K.; Tsogtbaatar, J.; et al. Carbon pool densities and a first estimate of the total carbon pool in the Mongolian forest-steppe. *Glob. Chang. Biol.* **2016**, *22*, 830–844. [CrossRef] [PubMed]
13. Dorjsuren, C.; Tungalag, M. Forest Status and Change of Mongolia. *Nat. Environ. Mong. Ulaanbaatar* **2017**, *3*, 221–246. (In Mongolian)
14. Krasnoshekov, Y.N. Features of the functioning and protective role of the forests of Mongolia. *Geogr. Nat. Resour. Russ.* **2001**, *1*, 135–142. (In Russian)
15. Krasnoshekov, Y.N. *The Soil-Protective Role of the Forests in the Basin of the Lake Baikal*; Publishing House of SB RAS: Novosibirsk, Russia, 2004; p. 224. (In Russian)
16. Dugarjav, C. *Larch Forests of Mongolia*; Bembi San Printing: Ulaanbaatar, Mongolia, 2006; p. 250, (In Mongolian with English summary).
17. Dorjsuren, C. Anthropogenic Successions of Larch Forest in Mongolia. In *Biological Resources and Natural Environment of Mongolia: Proceedings of the Joint Russian-Mongolian Complex Biological Expedition*; Russian Agricultural Academic Press: Moscow, Russia, 2009; Volume 50, p. 209. (In Russian with English summary)
18. Danilin, I.M. Structure and biomass of larch stand to regenerate naturally after clearcut logging. *Water Air Soil Pollut.* **1995**, *82*, 125–131. [CrossRef]

19. Chuluunbaatar, T. The relation between forest fuel and stand evaluation indication of subtaiga forest in northern Mongolia. In Proceedings of the Ecosystems of Mongolia and Frontier Areas of Adjacent Countries: Natural Resources, Biodiversity and Ecological Prospects: Proceeding of the International Conference, Ulaanbaatar, Mongolia, 5–9 September 2005; pp. 69–71.
20. Danilin, I.M.; Tsogt, Z. Morphometric parameters and phytomas of the Siberian larch *Larix sibirica* Ledeb. trees in the Eastern Khentey (Northern Mongolia). *Sib. J. For. Sci.* **2015**, *5*, 96–104. (In Russian with English abstract)
21. Battulga, P.; Tsogtbaatar, J.; Dulamsuren, C.; Hauck, M. Equations for estimating the above-ground biomass of *Larix sibirica* in the forest-steppe of Mongolia. *J. For. Res.* **2013**, *24*, 431–437. [CrossRef]
22. Dulamsuren, C.; Klinge, M.; Bat-Enerel, B.; Ariunbaatar, T.; Tuya, D. Effects of forest fragmentation on organic carbon pool densities in the Mongolian forest-steppe. *For. Ecol. Manag.* **2019**, *433*, 780–788. [CrossRef]
23. *Climate Reference Book of Mongolian People's Republic*; State Printing House: Ulaanbaatar, Mongolia, 1971; Volume I. (In Mongolian)
24. Korotkov, I.A. Forest type of the Mongolian People's Republic. Forests of the Mongolian People's Republic (Geography and Typology). In *Biological Resources and Natural Environment of Mongolia: Proceedings of the Joint Russian-Mongolian Complex Biological Expedition*; Nauka: Moscow, Russia, 1978; Volume 11, pp. 47–122. (In Russian)
25. Hosoda, K.; Iehara, T. Aboveground biomass equations for individual trees of *Cryptomeria japonica*, *Chamaecyparis obtusa* and *Larix kaempferi* in Japan. *J. For. Res. Jpn.* **2010**, *15*, 299–306. [CrossRef]
26. Dong, L.; Zhang, L.; Li, F. Developing additive systems of biomass equations for nine hardwood species in Northeast China. *Trees* **2015**, *29*, 1149–1163. [CrossRef]
27. Xue, Y.; Yang, Z.; Wang, X.; Lin, Z.; Li, D.; Su, S. Tree biomass allocation and its model Additivity for *Casuarina equisetifolia* in a tropical forest of Hainan Island, China. *PLoS ONE* **2016**, *11*, 1–20. [CrossRef]
28. Baskerville, G.L. Use of logarithmic regression in the estimation of plant biomass. *Can. J. Forest Res.* **1972**, *2*, 49–53. [CrossRef]
29. Overman, J.P.M.; Witte, H.J.; Saldarriaga, J.G. Evaluation of regression models for above-ground biomass determination in Amazon rainforest. *J. Trop. Ecol.* **1994**, *10*, 207–218. [CrossRef]
30. Packard, G.C.; Birchard, G.F.; Boardman, T.J. Fitting statistical models in bivariate allometry. *Biol. Rev.* **1994**, *86*, 549–563. [CrossRef] [PubMed]
31. Zeng, W.S.; Tang, S.Z. Modeling compatible single-tree aboveground biomass equations for masson pine (*Pinus massoniana*) in southern China. *J. For. Res.* **2012**, *23*, 593–598. [CrossRef]
32. Zianis, D.; Muukkonen, P.; Mäkipää, R.; Mecuccini, M. Biomass and stem volume equations for tree species in Europe. *Silva Fenn. Monogr.* **2005**, *4*, 1–63.
33. Cienciala, E.; Černý, M.; Tatarinov, F.; Apltauer, J.; Exnerová, Z. Biomass functions applicable to Scots pine. *Trees* **2006**, *20*, 483–495. [CrossRef]
34. Snowdon, P. A ratio estimator for bias correction in logarithmic regressions. *Can. J. For. Res.* **1991**, *21*, 720–724. [CrossRef]
35. Feng, Q.S.; Gao, X.H. Application of Excel in the Experiment Teaching of Leave-one-out Cross Validation. *Exp. Sci. Technol.* **2015**, *13*, 49–51, (In Chinese with English abstract).
36. Stone, M. Cross—validatory choice and assessment of statistical predictions. *J. R. Stat. Soc. Ser. B (Methodological)* **1974**, *36*, 111–147. [CrossRef]
37. Ruiz-Peinado, R.; Montero, G.; Monterodel Rio, M. Biomass models to estimate carbon stocks for hardwood tree species. *For. Syst.* **2012**, *21*, 42–52. [CrossRef]
38. Vargas-Larreta, B.; López-Sánchez, C.A.; Corral-Rivas, J.J.; López-Martínez, J.O.; Aguirre-Calderón, C.G.; Álvarez-González, J.G. Allometric equations for estimating biomass and carbon stocks in the temperate forests of North-Western Mexico. *Forests* **2017**, *8*, 269. [CrossRef]
39. Peichl, M.; Arain, A. Allometry and partitioning of above and belowground tree biomass in an aged sequence of white pine forests. *For. Ecol. Manag.* **2007**, *253*, 68–80. [CrossRef]
40. Sheil, D.; Eastaugh, C.S.; Vlam, M.; Zuidema, P.A.; Groenendijk, P.; Sleen, P.V.D.; Jay, A.; Vanclay, J. Does biomass growth increase in the largest trees? Flaws, fallacies and alternative analyses. *Funct. Ecol.* **2017**, *31*, 568–581. [CrossRef]

41. Köhl, M.; Neupane, P.R.; Lotfiomran, N. The impact of tree age on biomass growth and carbon accumulation capacity: A retrospective analysis using tree ring data of three tropical tree species grown in natural forests of Suriname. *PLoS ONE* **2017**, *12*, 1–17. [CrossRef] [PubMed]
42. Zhu, J.; Hu, H.; Tao, S.; Chi, X.; Li, P.; Jiang, L.; Li, C.; Zhu, J.; Tang, Z.; Pan, Y.; et al. Carbon stocks and changes of dead organic matter in China's forests. *Nat. Commun.* **2017**, *8*, 151. [CrossRef] [PubMed]
43. Wang, C. Biomass allometric equations for 10 co-occurring tree species in Chinese temperate forests. *For. Ecol. Manag.* **2006**, *222*, 9–16. [CrossRef]
44. Carvalho, J.P.; Parresol, B.R. Additivity in tree biomass components of Pyrenean oak (*Quercus pyrenaica* Willd.). *For. Ecol. Manag.* **2003**, *179*, 269–276. [CrossRef]
45. Bi, H.; Turner, J.; Lambert, M. Additive biomass equations for native eucalypt forest trees of temperate Australia. *Trees* **2004**, *18*, 467–479. [CrossRef]
46. Li, H.; Zhao, P. Improving the accuracy of tree-level aboveground biomass equations with height classification at a large regional scale. *For. Ecol. Manag.* **2013**, *289*, 153–163. [CrossRef]
47. Menéndez-Miguélez, M.; Canga, E.; Barrio-Anta, M.; Majada, J.; Álvarez-Álvarez, P. A three level system for estimating the biomass of *Castanea sativa* Mill. coppice stands in north-west Spain. *For. Ecol. Manag.* **2013**, *291*, 417–426. [CrossRef]
48. Sharifi, A.; Amini, J.; Pourshakouri, F. Allometric model development for Above-Ground Biomass estimation in Hyrcanian forests of Iran. *World Appl. Sci. J.* **2013**, *28*, 1322–1330.
49. Usoltsev, V.A.; Chasovskikh, V.P.; Noritsina, Y.V.; Noritsin, D.V. Allometric models of tree biomass for airborne laser scanning and ground inventory of carbon pool in the forests of Eurasia: Comparative analysis. *Sib. J. For. Sci.* **2016**, *4*, 68–76. (In Russian with English abstract)
50. Kozak, A. Methods for ensuring additivity of biomass components by regression analysis. *For. Chron.* **1970**, *46*, 402–405. [CrossRef]
51. Parresol, B.R. Assessing tree and stand biomass: A review with examples and critical comparison. *For. Sci.* **1999**, *45*, 573–593.
52. Tang, S.; Zhang, H.; Xu, H. Study on establish and estimate method of compatible biomass model. *Sci. Silvae Sin.* **2000**, *36*, 19–27, (In Chinese with English abstract).
53. Parresol, B.R. Additivity of nonlinear biomass equations. *Can. J. For. Res.* **2001**, *31*, 865–878. [CrossRef]
54. Dong, L.; Zhang, L.; Li, F. A three-step proportional weighting system of nonlinear biomass equations. *For. Sci.* **2015**, *61*, 35–45. [CrossRef]
55. Usoltsev, B.A. On additive models of tree biomass: Some uncertainties and the attempt of their analytical review. *Ecopotential* **2017**, *2*, 23–46.